TAP: Targeting and analysis pipeline for optimization and verification of coil placement in transcranial magnetic stimulation

Moritz Dannhauer [a], Ziping Huang [a,e], Lysianne Beynel [a], Eleanor Wood [a], Noreen Bukhari-Parlakturk [b], Angel V. Peterchev [a, c, d, e, *]

[a] Department of Psychiatry and Behavioral Sciences, Duke University, Durham, NC 27710, USA

[b] Department of Neurology, Duke University, Durham, NC 27705, USA

[c] Department of Electrical and Computer Engineering, Duke University, Durham, NC 27708, USA

[d] Department of Neurosurgery, Duke University, Durham, NC 27710, USA

[e] Department of Biomedical Engineering, Duke University, Durham, NC 27708, USA

[*] Corresponding author. E-mail: angel.peterchev@duke.edu

Conflict of Interest Disclosure

A. V. Peterchev has received research funding, travel support, patent royalties, consulting fees, equipment loans, hardware donations, and/or patent application support related to magnetic stimulation from Rogue Research, Tal Medical/Neurex, Magstim, MagVenture, Neuronetics, BTL Industries, and Advise Connect Inspire. The other co-authors report no relevant disclosures.

Funding

This work was supported by grants from the National Institutes of Health (RF1MH114268, RF1MH114253, U01AG050618, KL2TR002554), Dystonia Medical Research Foundation, Doris Duke Charitable Foundation, and Dystonia Coalition. The content is solely the responsibility of the authors and does not necessarily represent the official views of the funding agencies.

Data & Code Availability

The software described herein as well as resulting data to recreate all figures are available on https://github.com/moritzdannhauer/fMRI-based_TMS_Targeting_Pipeline.git.

Ethics Approval, Patient Consent, and Clinical Trial Registration

The human subjects participating in the fMRI and TMS experiments were part of a multi-session study of dystonia, including structural and functional magnetic resonance imaging and behavioral testing. The study was approved by the Duke University Health System Institutional Review Board (#0094131) ensuring ethical guidelines were followed and all subjects provided written informed consent to participate. The study was not registered as a clinical trial since it was a small pilot feasibility study and, moreover, this paper focuses on methodological aspects of TMS targeting and does not report any clinical results.

Abstract:

Transcranial magnetic stimulation (TMS) offers possibilities to modulate function in regions of interest (ROI) in the brain via an induced electric field (E-field). The ROI E-field can be maximized using individualized computational head modeling to find an optimal scalp coil placement. We present a TMS targeting and analysis pipeline (TAP) software that uses an MRI/fMRI-derived brain target to optimize a coil placement considering experimental requirements such as subject's hair thickness and coil placement restriction. The coil placement optimization is implemented in SimNIBS 3.2 for which an additional graphical user interface (TargetingNavigator) is provided to visualize and adjust procedural parameters. The optimized coil placement information is prepared for neuronavigation software (Brainsight) which supports the targeting during the TMS experiment. The neuronavigation system can record the coil placement during the experiment and these data can be processed in TAP to evaluate retrospectively and visualize the TMS targeting accuracy.

Keywords: TMS, MRI, coil, electric field, model, neuronavigation, targeting

1. Introduction

Precise placement of non-invasive brain stimulation devices, such as transcranial magnetic stimulation (TMS), offers promising avenues to understand basic (e.g., Jung et al., 2020) and higher (e.g., Beynel et al., 2020) cognitive brain functions. In neuroscience experiments, TMS coil placement is often landmark-referenced and supported by neuronavigation technology (Goetz et al., 2019; Rusjan et al., 2010), targeting a particular brain region of interest (ROI). These ROIs can be determined individually by identifying anatomical brain structures and their connectivity with MRI (Rusjan et al., 2010; Nummenmaa et al., 2014; Silva et al., 2020) or from the brain activity or functional connectivity obtained with fMRI or EEG (Wang et al., 2014; Bergmann et al., 2016; Zrenner et al., 2016; Thut et al., 2017; Curtin et al., 2019; Balderston et al., 2020; Beynel et al., 2020; Cash et al., 2020; Ding et al., 2020; Esposito et al., 2020; Zhang et al., 2020).

Prior to a TMS session, individualized computational modeling of head tissues and the electric field (E-field) induced in the ROI (Gomez et al., 2020) allows for identification of an optimal TMS coil placement on the scalp (Balderston et al., 2020; Gomez et al., 2021). We previously developed the fast auxiliary dipole method (ADM) for software-assisted TMS targeting to maximize E-field delivery to an ROI (Gomez et al., 2021), and ADM is now part of the SimNIBS E-field simulation software package (Thielscher et al., 2015). However, it remains challenging to combine ADM with individual functional or anatomical targeting data, subsequent experimental application using neuronavigation, and visualization and evaluation of the experimental accuracy. Previous publications proposed proof-of-principle fMRI-based TMS targeting pipelines (Balderston et al., 2020; Opitz et al., 2016). These efforts, however, have

several limitations with regard to coordinate transformations across software packages, coil placement constraints and optimization, inclusion of hair thickness information, user interface for verification of ROI input information, and retrospective validation of TMS coil placement accuracy.

We present a TMS targeting and analysis pipeline (TAP) software that helps bridge the gaps between individual imaging data, SimNIBS, and neuronavigation. SimNIBS can robustly generate head tissue models (Thielscher et al., 2015) from MRI data. The ADM method in SimNIBS finds the optimal TMS coil position and orientation on each subject's scalp to maximize the magnitude or a directional component of the ROI E-field (Gomez et al., 2021). To add to SimNIBS' basic functionality for adjustment and visualization of ROIs, the coil, and desired E-field parameters, TAP offers a graphical user interface (GUI), called 'TargetingNavigator'.

TAP can be used for prospective targeting optimization before an experiment and/or retrospective targeting analysis after an experiment. The first step, in a prospective approach for TMS coil placement or E-field simulation, is to extract an ROI center from a volumetric target mask (i.e., a nifti file) for SimNIBS. In this approach, TAP generates specifically formatted ASCII text files readable by the TMS neuronavigation software (Brainsight, 2020). The presented implementation is for the Brainsight neuronavigation system, but TAP can be adapted to other systems as well. TAP can also control practical aspects of the coil placement such as the coil handle direction, which ideally should not block the TMS coil tracker or the subject's sight and which may need adjustment to control the induced E-field direction in the cortex (Brasil-

Neto et al., 1992; Balslev et al., 2007). Retrospective analysis uses TMS coil placement data from an existing experiment recorded by neuronavigation software. In retrospective analysis, TAP can detect problematic coil distances from the scalp, such as a coil placement being too far from or entering the scalp surface due to inaccurate coil–scalp co-registration, or movement of the TMS coil during the stimulation; this analysis can incorporate measurements of the subjects' hair thickness (Beynel et al., 2020), if such are available.

In this paper, we describe TAP and illustrate its use in five TMS subjects who participated in a study of writer's cramp dystonia.

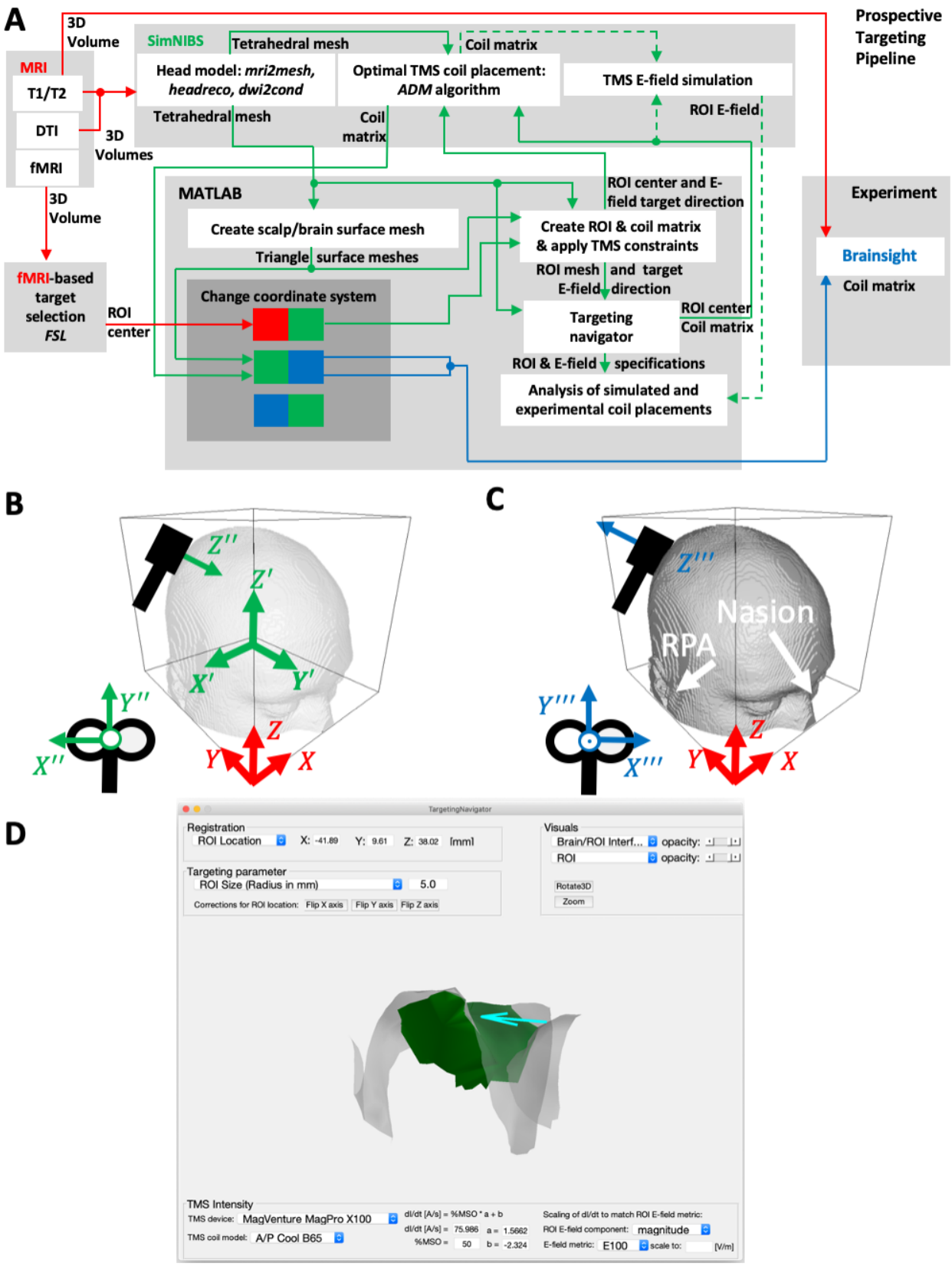
A
Prospective Targeting Pipeline
3D Volume
MRI
T1/T2
DTI
fMRI
3D Volumes
3D Volume
fMRI-based target selection FSL
ROI center
SimNIBS
Tetrahedral mesh
Coil matrix
Head model: mri2mesh, headreco, dwi2cond
Optimal TMS coil placement: ADM algorithm
TMS E-field simulation
Tetrahedral mesh
Coil matrix
ROI E-field
MATLAB
ROI center and E-field target direction
Create scalp/brain surface mesh
Triangle surface meshes
Create ROI & coil matrix & apply TMS constraints
ROI mesh and target E-field direction
Change coordinate system
Targeting navigator
ROI center
Coil matrix
ROI & E-field specifications
Analysis of simulated and experimental coil placements
Experiment
Brainsight
Coil matrix
B
Z''
Z'
X'
Y'
Y''
X''
Z
Y
X
C
Z'''
Nasion
RPA
Y'''
X'''
Z
Y
X
D
TargetingNavigator
Registration
ROI Location
X: -41.89
Y: 9.61
Z: 38.02
[mm]
Targeting parameter
ROI Size (Radius in mm)
5.0
Corrections for ROI location:
Flip X axis
Flip Y axis
Flip Z axis
Visuals
Brain/ROI Interf...
opacity:
ROI
opacity:
Rotate3D
Zoom
TMS Intensity
TMS device:
MagVenture MagPro X100
TMS coil model:
A/P Cool B65
dI/dt [A/s] = %MSO * a + b
dI/dt [A/s] = 75.986
a = 1.5662
%MSO = 50
b = -2.324
Scaling of dI/dt to match ROI E-field metric:
ROI E-field component:
magnitude
E-field metric:
E100
scale to:
[V/m]

Figure 1. (A) Diagram of the TMS targeting and analysis pipeline (TAP) integrating different hardware and software components for prospective targeting. The dashed arrows indicate optional steps that are not required for prospective targeting. (B) SimNIBS software coordinate convention (green) with origin at the volumetric center, X' and Y' axes flipped with respect to the MRI RAI convention (X, Y, Z, in red), and a TMS coil coordinate system (X''', Y''', Z'''). (C) Brainsight neuronavigation coordinate convention (blue) with pitch $X''' = -X''$ and yaw $Z''' = -Z''$ flipped compared to the SimNIBS convention. The nasion and right/left periauricular points (RPA/LPA) are typical registration points for neuronavigation. (D) A screenshot of the TargetingNavigator GUI: a MATLAB-based SimNIBS 3.2 add-on to adjust and visualize simulation parameters in prospective and retrospective TMS analysis.

2. Material and methods

As diagrammed in Figure 1A, TAP combines existing software packages, including SimNIBS v3.2 (Thielscher et al., 2015) for TMS-induced E-field simulations and Brainsight v2.5b2 (Brainsight, 2020) for neuronavigation, with custom MATLAB R2018a code (MathWorks, 2018). The following sections describe how TAP was utilized in a complex study paradigm. Briefly, individual TMS target ROIs were derived from fMRI (section 2.1), optimal coil placements were computed prospectively (section 2.2) and applied in experimental TMS sessions (section 2.3), and the experimental coil placements were recorded and analyzed to assess the targeting accuracy (section 2.4).

2.1 Experimental participants, MRI, and target selection

2.1.1 Participants

The study (Bukhari-Parlakturk et al., 2021) was open to all patients with writer's cramp (WC) dystonia in their right hand who were not on any symptomatic treatments for more than three months and had no contraindications to MRI and TMS. Age-matched healthy volunteers (HV) who were right hand dominant with no brain disorders were also recruited for the research study. Thirteen WC and 13 HV consented and completed the fMRI visit and of these, five subjects (4 WC and 1 HV) consented and completed the three TMS visits as detailed below.

2.1.2 fMRI research design

All subjects completed a writing task in the MRI scanner during which they were presented with visual instructions to copy a sentence on an MRI compatible digital tablet. The fMRI acquisition lasted for approximately 7.5 minutes and comprised twelve 20-second blocks of writing separated by periods of rest.

2.1.3 Image acquisition and preprocessing

A total of 13 WC and 13 HV completed structural MRI and functional MRI (fMRI) sequences. A 3 Tesla GE scanner was used to collect structural T1-weighted (echo-planar sequence: voxel size = $1 \times 1 \times 1.3$ mm^3, TR (repetition time) = 6.836 s; TE (echo time) = 2.976 s; FOV (field of view) = 25.6 mm^2, bandwidth 41.67 Hz/pixel), T2-weighted (echo-planar sequence voxel size = $1 \times 1 \times 1.3$ mm^3, TR = 1267.0 ms, TE = 20 ms, flip angle 10°, FOV = 25.6 mm^2, bandwidth 31.26 Hz/pixel) and diffusion-weighted scans (voxel size = $1 \times 1 \times 1.3$ mm^3, TR = 9000 ms, TE = 92.1 ms, FOV = 25.6 mm, bandwidth 250 Hz/pixel, matrix size 128×128, B-value = 2000 s/mm^2,

diffusion direction = 36). Functional echo-planar images were acquired while subjects performed the writing task using the following parameters: voxel size = 3.5 × 3.5 × 4.0 mm^3, TR = 2 s, TE = 30 ms, flip angle = 90°, FOV = 22 cm, bandwidth = 250 Hz/Pixel, interleaved slice order with whole brain coverage). The Cigal software was used to align each subject's movement to a reference frame to monitor movement in real time (Voyvodic, 1999). All fMRI images were preprocessed using the fMRIPrep software after discarding first 5 brain volumes (Esteban et al., 2019).

2.1.4 TMS target selection

Preprocessed fMRI sequences were imported into the FSL software (Jenkinson et al., 2012; available at https://fsl.fmrib.ox.ac.uk/fsl/fslwiki/) to perform general linear modeling (GLM) at the individual subject level (with spatial smoothing of 5 mm, cluster z-threshold of 2.3, and p-value of 0.05). The GLM model involved convolution of the writing blocks to the double-gamma hemodynamic response function to identify the regions of brain activation for each subject during the writing task compared to rest period (Jenkinson et al., 2012; Voyvodic, 1999). The z-stat brain activation maps of each subject's writing task were then moved into a second level group analysis using mixed effects FLAME1 modeling to generate the mean brain activation maps for 13 WC and for 13 HV subjects during the writing task. The z-stat brain activation maps for each of the 5 subjects (4 WC and 1 HV) were then visualized to develop customized ROIs for TMS stimulation. Specifically, each subject's activation map was overlaid on the respective group activation map and a mask of the structural left premotor cortex or the primary sensory cortex as defined by the Harvard-Oxford MNI atlas (Desikan et al., 2006). ROI targets for TMS were defined by selecting two neighboring voxels, which were within the atlas-

defined left premotor cortex or primary sensory cortex, had peak activation with z-statistic > 2.3, showed overlap between the individual and group activation maps, and were within 4 mm from the cortical surface. The 4 mm rule was used to ensure the cortical ROI can be reached by the TMS E-field (Aberra et al., 2020). The individual ROIs were then reversed transformed into individual native space using FLIRT linear registration with a sinc interpolation. The ROIs in the individual native MRI voxel space were then imported into the TAP workflow to identify the ROI center and transform to the computational model mesh (SimNIBS space) for determination of the optimal TMS coil placements.

2.2 TMS targeting and analysis pipeline (TAP)

2.2.1. Coordinate system transformations

Generally, coordinate transformations are needed to integrate all different software pieces (MRI, SimNIBS, and Brainsight) in the pipeline mediated by custom MATLAB code. The coordinate transformations are defined as 4 × 4 matrices (denoted as $T_{i,j}$ with $i, j = 1, \ldots, 4$) which contain submatrices for rotation ($T_{i,j}$ with $i, j = 1, 2, 3$) defining axes rotations (with $\|T_{*,j}\| = 1$ for $j = 1, 2, 3$) and translation ($T_{i,j}$ with $i = 1, 2, 3; j = 4$ in units of mm; $T_{4,4} = 1$) adding a coordinate offset that moves the origin of a current coordinate system to the specified desired one. The matrix $T_{i,j}$ is used to map locations such as the ROI and the TMS coil center, coordinate space rotations (i.e., colored arrows or letters in Figure 1A–C), and coil coordinate transformations from neuronavigation (Brainsight, 2020) or canonical coil space into SimNIBS modeling space (Thielscher et al., 2015), denoted as 'Coil matrix' in Figure 1A. The coordinate system transformations from MRI or Brainsight to SimNIBS space are performed based upon mapping

coordinates (expressed as world coordinates) relative to the center of the image volume of the respective MRI file created with SimNIBS (*SubjectName_T1fs_conform.nii.gz*) using either the *mri2mesh* or *headreco* pipeline. In more detail, *SubjectName_T1fs_conform.nii.gz* is present in the RPI (radiological standard) coordinate/voxel-order system (except for the *headreco* option *non-conform* where it keeps the coordinate system of the input MRI), where the origin is at the RPI corner of the voxel space with positive voxel X, Y and Z axes, respectively. A 4 × 4 transformation matrix or quaternion transformation is stored in either MRI or ROI-defining image file (nifti file, extension: *nii.gz*) with additional information which is used by default transforming voxel coordinates to world coordinates. The nifti-header information can be modified by a variety image processing software and some may transform any image to one specific voxel-order/coordinate system (e.g., to the RAI in Seg3D, (CIBC, 2015)) creating the appearance of being at a proper location. To ensure the correctness of the transformed ROI coordinate, TAP computes the shortest Euclidean distance to the next segmented gray matter volume in SimNIBS MRI-space (i.e., 'SubjectName_T1fs_conform.nii.gz') using 'gm_fromMesh.nii.gz' SimNIBS v3 or 'gm_only.nii.gz' for SimNIBS v2 mri2mesh runs. If this distance is larger than the voxel size, then the ROI and gray matter do not overlap. In that problematic case, which is most likely due to voxel-order/coordinate transformation misalignment, TAP can be either configured to systematically sign-flip the axes/origin to find a world coordinate transformation with minimal distance or do that manually by starting the TargetingNavigator for inspection and adjustment.

Once the ROI voxels are in SimNIBS MRI-space (i.e., in *SubjectName_T1fs_conform.nii.gz*) as world coordinates (X, Y, Z), they need to be converted to SimNIBS model-space (X', Y', Z') by

representing the coordinates relative to the image center and flip axis ($X' = -X, Y' = -Y, Z' = Z$, see Figure 1B). The physical orientation of the TMS coil is defined in SimNIBS space (denoted X'', Y'', Z'') and Brainsight space (denoted as X''', Y''', Z'''), while flipping by 180º the pitch ($X''' = -X''$) and yaw coil orientation axes (i.e., $Z''' = -Z''$). Coil orientations are then visualized by black-colored coil representations in Figure 1B and 1C respectively. For biphasic TMS pulses, TMS is most effective when the direction of the middle phase of the induced E-field is pointing into the wall of the cortical sulci (Corthout et al., 2001; Kammer et al., 2001; Balslev et al., 2007; Beynel et al., 2020). As described in section 'Preparation and launch of SimNIBS', TAP estimates this direction based on the gyral/sulcal transition zone in the ROI (i.e., through cortical curvature information in SimNIBS mri2mesh; for more details see below) to find a representative location on the wall for which it computes a smoothed inward-pointing normal vector. This vector is then used as the ROI directional E-field constraint in ADM to find the optimal TMS coil setup. After ADM has finished, the optimal coil orientation is prepared for Brainsight considering the following experimental constraints. The Z''' axis is checked for pointing in the scalp-outward direction (indicated visually by a large green cylinder cone in Brainsight). Further, for TMS devices that allow electronic reversal of the coil current direction, there is the option to flip the coil orientation and current direction for most practical experimental coil placement. It is advantageous to keep the orientation of the TMS coil handle, including any attached cable, pointing away from the subject's face and TMS tracking headgear. To achieve this, TAP projects the optimized TMS coil orientation (Y'') onto the anterior–posterior ($X' - Z'$) plane and then computes an angle α with the X' axis (equals zero-degree axis and positive angles for clockwise rotation). If 90° < α < 270°, then the coil orientation is flipped, and the necessity for coil current reversal is highlighted in the prepared Brainsight files.

2.2.2 Preparation and launch of SimNIBS

TMS coil placement optimization can be launched with TAP by executing the *run_simnibs(s)* command from the MATLAB prompt providing a MATLAB struct object *s* with different data fields, which should be initialized with the default struct *opt_struct('TMSoptimize')*.

If *s* has the data field entry *s.target_direction*, ADM or the direct solver in SimNIBS will find the coil placement that maximizes the average E-field induced in the ROI along *s.target_direction*, or otherwise the overall magnitude, as specified. The ROI center location in SimNIBS space is assigned to data field *s.target*. The ROI size (*s.target_size*) considers all tetrahedral gray matter elements that fall within this radius (from the point specified in *s.target*). For our five TMS subjects, an ROI size value between 3–4 mm was chosen to ensure the ROI covers a significant part of the sulcal wall but not any part of a neighboring gyrus controlled for by visual inspection in TargetingNavigator. The ROI target direction is determined following these main steps:

(1) project the ROI center onto the smoothed brain surface;

(2) project location from (1) to the closest scalp surface mesh point and compute its nodal normal (averaging the neighboring triangle normal vectors) representing the coil plane;

(3) find sulcal wall location / trajectory (convex–concave transition of sulcus and gyrus):

(3.1) mri2mesh: use location from (1) and Freesurfer's surface curvature information (files: *lh.sulc*, *rh.sulc*; value range: between –2 and 2) to find the nearest surface mesh point that is numerically closest to zero;

(3.2) headreco: use location from (1) and its scalp projection to form a trajectory vector;

(4) compute an outwards-pointing nodal normal by averaging the triangle normal vectors for the brain surface nodes; and

(5) find sulcal wall surface normal and adjust for scalp coil plane

(5.1) mri2mesh: determine the nodal normal (4) for location (3.1)

(5.2) headreco: move up/down the trajectory vector to find a location for which its nodal normal is mostly parallel to the tangential plane at the closest scalp node (2).

The sulcal wall normal vector found in (5) for mri2mesh or headreco, respectively, is then adjusted by projection onto the tangential plane (using the closest scalp node normal vector) to create the desired ROI target direction vector, since the TMS induced E-field is mostly tangential to the scalp surface.

For robust estimation of the scalp-tangential plane, we added a data field to the *s* structure (available in SimNIBS 3.2.5), namely *s.scalp_normals_smoothing_steps* (TAP default is 20), to adjust the coil tangentiality to the scalp and visualize it in TargetingNavigator.

SimNIBS allows constraining the scalp search space for possible coil center positions and orientations, which TAP sets to the default values of *s.search_radius* = 25 mm, *s.spatial_resolution* = 1 mm and *s.search_angle* = 1°. For a typical SimNIBS head model and those default values, the optimal coil placement search takes about 2 minutes on a regular laptop (Intel Core i5 1.6 GHz, 8 GB RAM) running ADM.

2.2.3. Prospective TMS dosing

For the five TMS subjects, we used mri2mesh/dwi2cond (SimNIBS 2.0.1) to generate a five-tissue head model from the subject's T1-weighted MRI data set, and assign to the resulting tetrahedral mesh elements isotropic conductivities for the scalp (0.465 S/m), skull (0.01 S/m),

and cerebrospinal fluid (1.654 S/m), as well as anisotropic conductivities for the gray and white brain matter. The anisotropic conductivities were derived from the subject's co-registered diffusion-weighted MRI, where the diffusion tensors are volume-normalized so that the geometric mean of the conductivity tensor eigenvalues equals literature-based values of 0.275 S/m and 0.126 S/m for gray and white matter, respectively.

The subject's hair thickness is often unknown before the TMS session but can be measured at the beginning of the session (Beynel et al., 2020). Therefore, multiple runs of SimNIBS's ADM are required for a range of hair thickness values. The default setting in TAP iterates through a reasonable range of hair thicknesses from 0 to 7.5 mm in steps of 0.5 mm. The optimal coil setup is chosen for TMS targeting (i.e., as loaded into Brainsight) while a TMS intensity related to the subject's resting motor threshold was employed as described in section 2.3.

The TMS pulse intensity, specified as the coil current rate of change (*dI/dt*), can be set as a parameter directly in SimNIBS (default: *s.didt* = 10^6 A/s = 1 A/µs) or through the TargetingNavigator interface. TAP also offers the option to determine the needed *dI/dt* to reach a desired E-field strength in the ROI—an important feature for ROI-based dosing of TMS. The desired directional or magnitude E-field strength in the ROI can be specified in TAP by one of several metrics: the maximal value as well as statistically more robust metrics, such as the 50th, 75th, 90th and 99th percentile, to avoid numerical E-field outliers. Available are also our previously proposed E20, E50 and E100 metrics which define the minimum E-field strength respectively within the 20, 50, and 100 voxels with strongest E-field in the ROI (Beynel et al., 2020, 2021). The computed *dI/dt* can be entered into the TMS device, typically as percentage of

the maximum stimulator output (%MSO), based on the approximately linear relationship between *dI/dt* and %MSO (Beynel et al., 2020, 2021). This realtionship can be described generally by the formula

$$\frac{dI}{dt} = \%\text{MSO} \cdot a + b \tag{1}$$

where coefficients a and b can be fitted to empirical data, obtained, for example, from TMS devices that provide both %MSO and *dI/dt* [A/µs] readout. In that case, *dI/dt* should be measured across the full range of intensity for a specific coil, for example with 5% MSO steps (Beynel et al., 2020, 2021). For devices that do not display *dI/dt*, the most practical approach is to set $b = 0$, and compute

$$a = \frac{V_{c,max}}{100 \cdot L} \tag{2}$$

from the TMS device maximum capacitor voltage, $V_{C,max}$, corresponding to 100 %MSO, and the specific coil inductance L, both of which can be obtained from the manufacturer. For example, $V_{C,max}$ is 1,800 V, 1,670 V, and 2,800 V for standard MagVenture MagPro, Magstim Rapid[2], and Magstim 200[2] devices, respectively. The Targeting Navigator interface incorporates the ability to solve equation (1) for either *dI/dt* or %MSO with specified a and b, and provides values for these coefficients for some common TMS device and coil combinations.

2.2.4. Neuronavigation files

TAP generates different types of files that can then be visualized in Brainsight:

(1) scalp and brain surface of the SimNIBS head model converted to MRI/Brainsight space,

(2) SimNIBS/Freesurfer preprocessed T1-weighted MRI data set,

(3) ROI/scalp coil center converted to MRI/Brainsight space, and

(4) optimal coil placement (fully defined by a 4 × 4 matrix) converted to Brainsight space and saved in a text file.

For retrospective analysis, the experimenter can save the coil placement data as text files (i.e., for Brainsight software) during the TMS session, which can then be read into MATLAB and visualized in TargetingNavigator.

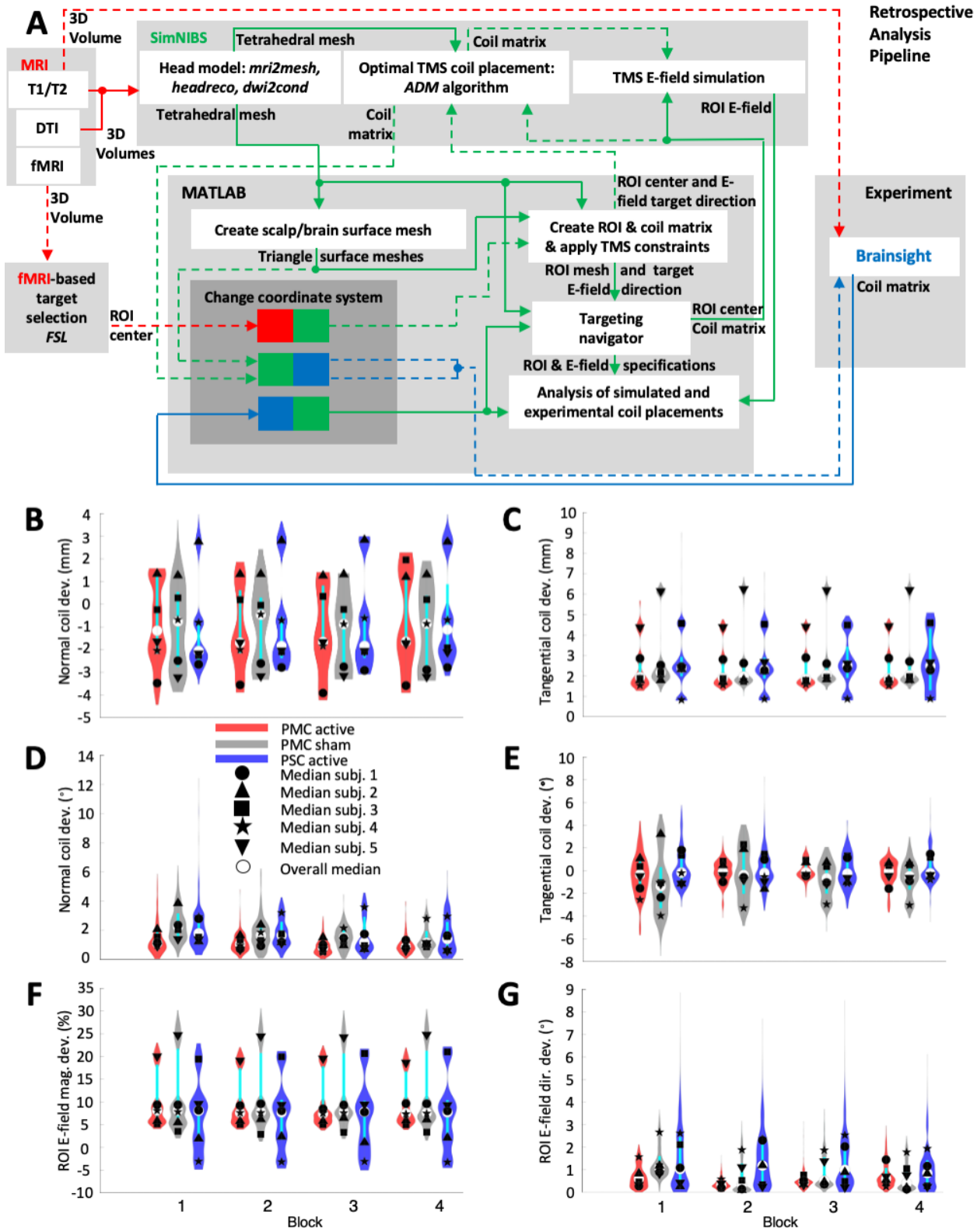
A
Retrospective Analysis Pipeline
3D Volume
MRI
T1/T2
DTI
fMRI
3D Volumes
3D Volume
fMRI-based target selection FSL
ROI center
SimNIBS
Tetrahedral mesh
Head model: mri2mesh, headreco, dwi2cond
Tetrahedral mesh
Coil matrix
Optimal TMS coil placement: ADM algorithm
Coil matrix
TMS E-field simulation
ROI E-field
MATLAB
Create scalp/brain surface mesh
Triangle surface meshes
Change coordinate system
ROI center and E-field target direction
Create ROI & coil matrix & apply TMS constraints
ROI mesh and E-field target direction
Targeting navigator
ROI center
Coil matrix
ROI & E-field specifications
Analysis of simulated and experimental coil placements
Experiment
Brainsight
Coil matrix
B
Normal coil dev. (mm)
C
Tangential coil dev. (mm)
D
Normal coil dev. (°)
E
Tangential coil dev. (°)
F
ROI E-field mag. dev. (%)
G
ROI E-field dir. dev. (°)
Block
PMC active
PMC sham
PSC active
Median subj. 1
Median subj. 2
Median subj. 3
Median subj. 4
Median subj. 5
Overall median

Figure 2. (A) Diagram of TAP as used for retrospective dosing analysis based on TMS coil scalp placement data recorded via Brainsight. Dashed arrows indicate optional steps that are not required for retrospective TMS analysis. (B)–(G) Violin plots and medians of the differences in coil placement and induced E-field between prospectively-optimized and neuronavigation-recorded targeting in 5 subjects for 3 rTMS sessions of 4 blocks each. Deviation distance of (B) the coil center along the coil normal (yaw axis) direction (positive/negative values represent coil surface above/below the scalp surface) and (C) the coil center in the plane tangential to the scalp. Angular deviation of (D) the coil normal (yaw axis) and (E) the coil orientation about its yaw axis with clockwise as the positive direction. (F) Magnitude and (G) angular deviation of the E-field vectors for each finite element in the ROI. The violin plots show the distribution of the data, with thin black and thicker cyan vertical lines representing the 95% confidence interval and the interquartile range, respectively (Bechthold, B., 2016). The plots exclude samples that have normal or tangential deviation distance of more than ± 10 mm, which were considered outliers that likely occurred due to brief disruptions in the coil tracking and comprised only 0.069% of the data.

2.3 Experimental TMS sessions

The optimal TMS coil placement information of the five subjects who received TMS was imported as a project file (comprising of PMC or PSC cortical target, T1, scalp conformation, and hair thickness estimations) into the Brainsight software for the TMS sessions. All TMS sessions were performed in a double-blind, sham-controlled, cross-over research design. Three TMS sessions per subject were performed in a randomized order: active TMS at premotor cortex, sham TMS at premotor cortex, and active TMS at primary sensory cortex, with each session one week apart to allow washout of the rTMS neuromodulatory effects. Each session was divided into 4 blocks, each 5 minutes apart. During each

block, subjects received 25 trains of 3.9 s, 10 Hz repetitive TMS with intertrain interval of 10 seconds at 90% resting motor threshold with biphasic stimulation for a total of 1,000 and 4,000 pulses per block and session, respectively. TMS was delivered using a MagPro X100 stimulator with A/P Cool-B65 coil (MagVenture, Alpharetta, GA, USA). A Neuronavigation system (Brainsight, Rogue Research, Montreal, Canada) was used to co-register the T1-MRI and the fMRI-based TMS target developed with TAP to the subject's scalp. Then, the location of the subject's hot spot over the left motor cortex that induced the strongest motor evoked potentials in the contralateral first dorsal interosseus (FDI) was determined and marked in Brainsight. The resting motor threshold (rMT, expressed as %MSO) was then determined using a maximum-likelihood-based estimation procedure (see Table 1) (Awiszus & Borckardt, 2011). The subject's hair thickness over the TMS target area was measured (see Table 1) (Beynel et al., 2020) and the closest hair thickness value in the reference table provided by TAP was selected. The TMS coil position and orientation values corresponding to the selected hair thickness were then used for each TMS session. During sham stimulation, the A/P coil was flipped, and subjects received similar auditory stimulation and scalp sensation through two surface electrodes placed on the subject's scalp around the TMS target producing only about 7.7% of the active E-field stimulation in the brain (Smith & Peterchev, 2018). For all TMS sessions, the experimenter positioned the coil tangentially to the scalp surface with its handle directed posteriorly with goal angle deviation < 5º. The coil placement data were saved by Brainsight every 500 ms (every fifth pulse) during the rTMS trains, totaling 200 recorded TMS coil setups per block, and exported as text files. Recording the coil position at this reduced rate compared to the pulse train rate was necessary for the neuronavigation system (Brainsight) to be able to correctly save all data points. No adverse events due to the stimulation were reported.

Subject	rTMS intensity setting (% MSO)			Hair thickness (mm)		
	Session target & TMS condition			Session target & TMS condition		
	PMC Sham	PMC Active	PSC Active	PMC Sham	PMC Active	PSC Active
S1	52	53	47	0.5	0.5	0.5
S2	76	69	64	2.5	2.0	2.5
S3	39	41	38	1.5	1.5	2.5
S4	46	50	47	2.0	2.5	2.0
S5	55	58	45	2.0	2.0	3.5

Table 1. rTMS intensity setting, equal to 90% of the individual resting motor threshold (rMT), and hair thickness measurement (in mm) of the five study subjects for the three TMS sessions (listed by target and TMS condition, not in chronological order).

2.4. Retrospective Analysis

The Brainsight neuronavigation system can digitize the coil position and orientation for each TMS pulse. TAP reads in (*read_brainsight_file*) the Brainsight-space exported text files and converts each line, corresponding to one digitized coil placement defined by a 4 × 4 transfer matrix, to SimNIBS modeling space (*convert_coord_brainsight_2_simnibs*). To avoid possible errors in the coil–scalp co-registration resulting in the coil center being inside the scalp, it is recommended to use Brainsight's "Snap to Scalp" option when exporting (Brainsight, 2020). TAP then extrudes these snapped coil centers outwards along the scalp normal to account for the measured hair thickness. If hair thickness measurement is unavailable, TAP defaults to a value of

2 mm (Beynel et al., 2020). The distance between the hair-thickness-extruded coil center and the original experimentally recorded coil center without snapping and hair-thickness extrusion is determined along the recorded coil normal direction ('normal coil deviation' in mm). The hair-thickness-extruded coil center is then compared against the computationally optimal coil center on the scalp's tangential plane ('tangential coil deviation' in mm). TAP uses the computationally optimal coil placement to also check if the rotational part of the experimental coil placement matrices aligns, and sign-flips the components for minimal angular discrepancy. The scalp normal direction is used to assess the deviation of the coil plane from the scalp-tangential plane ('normal coil deviation' in angular degree (°) equal to the arccosine of the dot product of the scalp and coil normal). Finally, the experimental coil placement is projected onto the scalp-tangential plane and the difference between the experimental and optimal coil orientation is computed ('tangential coil deviation' in angular degree (°)). When a targeted optimal coil placement is not available, TAP can still analyze the experimental TMS coil placements recorded with Brainsight.

As a second step, TAP evaluates the difference in induced E-field between the optimal (if one is provided) and all experimentally recorded coil setups. Since one E-field simulation requires several minutes of computation time, TAP avoids a very long total simulation time by choosing a median representative of the coil placements within an experimental block to simulate the E-field in the entire head model and then extracts the ROI E-field (using SimNIBS 'target.msh'). The median coil representation is chosen by evaluating the medians for the X''', Y''' and Z''' coordinates separately and picking the recorded coil placement with the smallest Euclidean distance from these median coordinates. For the E-field simulations, the value of *dI/dt* is

computed with Equation (1) from the individual rMT in units of %MSO, and entered into the *s.didt* field of the MATLAB structure inputted to SimNIBS. For the TMS coil and device in this study, coefficient values of $a = 1.5662$ and $b = -2.3237$ were used in Equation (1) based on prior calibration data (Beynel et al., 2020). Finally, TAP computes the deviation in magnitude and angle of the E-field vector in each tetrahedral ROI element between the simulations for the median experimental coil placement and the optimal coil placement.

4. Results

Figure 2B–G quantifies the deviation between the computationally optimized coil placement that was set as a target during the TMS sessions and the actual placements recorded by the neuronavigation system. Across all subjects and sessions, the median coil position and orientation deviations were −1.55 mm and 1.28° relative to the scalp normal (Figure 2B, D) and 2.18 mm and −0.29° in the scalp tangential plane (Figure 2C, E), respectively. The corresponding median E-field magnitude and direction deviations (Figure 2F,G) were 7.69% and 0.65°, respectively, even though some of the individual medians were significantly larger.

These values are comparable to neuronavigation error and deviation estimates in the literature. TMS neuronavigation systems are known to have a coil placement accuracy of 5–6 mm on average (FDA, 2020; Ruohonen & Karhu, 2010). Excluding errors from the registration and shifts of the head tracker relative to the head, median tangential deviation of the coil position and orientation of 1.34 mm and 3.48°, respectively, was reported for a neuronavigated robotic coil

holder (Goetz et al., 2019). Moreover, inter-session position error of about 2.5 mm was reported for neuronavigated manual coil placement (Schönfeldt-Lecuona et al., 2005).

5. Discussion and Conclusions

The novel targeting and analysis pipeline (TAP) integrates the SimNIBS E-field simulation package with the Brainsight neuronavigation system using custom MATLAB code to improve the practicality of precise brain targeting in TMS experiments using E-field simulations. TAP enables prospective and retrospective TMS targeting analysis based on E-field simulations coupled with individual imaging and neuronavigation data. Prospective targeting computations include the optimization of the TMS coil placement as well as, optionally, selecting the TMS pulse intensity to deliver a specific E-field strength at the target ROI. Retrospective analysis of the experimental coil placement can quantify the overall accuracy of applying TMS. For example, retrospective coil placement analysis can be used to remove problematic TMS sessions, blocks, or pulses, perform statistical analyses to explain experimental outcomes, and draw more accurate conclusions from hypothesis-driven TMS research. Thus, TAP offers capabilities to assess and enhance experimental reproducibility and ways to ensure scientific rigor. We demonstrated the use of TAP in an example study where it reported TMS coil positioning deviations not exceeding the error levels of neuronavigation systems.

TAP is an extension to SimNIBS, which is also freely available. It is our hope that TAP will enable more researchers to utilize the SimNIBS E-field simulation capabilities as part of rigorous TMS targeting and analysis methods. TAP also facilities readout from the Brainsight neuronavigation system to uncover potential issues regarding the coil placement, including coil tracking and/or head registration. Presently, the TAP code supports only Brainsight, but we aim

to make it compatible also with other neuronavigation systems in the future. Finally, we welcome input and contributions to the TAP code by users through the contact on the TAP GitHub page linked in section Data & Code Availability.

References

Aberra, A. S., Wang, B., Grill, W. M., & Peterchev, A. V. (2020). Simulation of transcranial magnetic stimulation in head model with morphologically-realistic cortical neurons. *Brain Stimulation*, *13*(1), 175–189.

Awiszus, F., & Borckardt, J. (2011). *TMS Motor Threshold Assessment Tool* ((MTAT 2.0)) [Computer software]. https://www.clinicalresearcher.org/software.htm

Balderston, N. L., Roberts, C., Beydler, E. M., Deng, Z.-D., Radman, T., Luber, B., Lisanby, S. H., Ernst, M., & Grillon, C. (2020). A generalized workflow for conducting electric field–optimized, fMRI-guided, transcranial magnetic stimulation. *Nature Protocols*, *15*(11), 3595–3614.

Balslev, D., Braet, W., McAllister, C., & Miall, R. C. (2007). Inter-individual variability in optimal current direction for transcranial magnetic stimulation of the motor cortex. *Journal of Neuroscience Methods*, *162*(1–2), 309–313.

Bechthold, B. (2016). *Violin Plots for Matlab* [MATLAB]. https://github.com/bastibe/Violinplot-Matlab,

Bergmann, T. O., Karabanov, A., Hartwigsen, G., Thielscher, A., & Siebner, H. R. (2016). Combining non-invasive transcranial brain stimulation with neuroimaging and electrophysiology: Current approaches and future perspectives. *Neuroimage*, *140*, 4–19.

Beynel, L., Dannhauer, M., Plamer, H., Hilbig, S. A., Crowell, C. A., Wang, J. E.-H., Micheal, A. M., Wood, E. A., Luber, B., Lisanby, S. H., Peterchev, A. V., Cabeza, R., Davis, S. W., & Appelbaum, L. G. (2021). *Network-based rTMS to modulate working memory: The difficult choice of effective parameters for online interventions. in press*.

Beynel, L., Davis, S. W., Crowell, C. A., Dannhauer, M., Lim, W., Palmer, H., Hilbig, S. A., Brito, A., Hile, C., Luber, B., Lisanby, S. H., Peterchev, A. V., Cabeza, R., & Appelbaum, L. G. (2020). Site-specific effects of online rTMS during a working memory task in healthy older adults. *Brain Sciences*, *10*(5), 255.

Brainsight, D. T. (2020). *Brainsight* (v2.5b3 (58023)) [MacOS]. Rogue Research Inc. https://www.rogue-research.com/downloads/

Brasil-Neto, J. P., Cohen, L. G., Panizza, M., Nilsson, J., Roth, B. J., & Hallett, M. (1992). Optimal focal transcranial magnetic activation of the human motor cortex: Effects of coil orientation, shape of the induced current pulse, and stimulus intensity. *Journal of Clinical Neurophysiology: Official Publication of the American Electroencephalographic Society*, *9*(1), 132–136.

Bukhari-Parlakturk, N., Fei, M., Voyvodic, J., & Michael, A. M. (2021). Data Driven Exploration of Network Connectivity in task-fMRI of Focal Hand Dystonia. *MedRxiv*.

Cash, R. F., Weigand, A., Zalesky, A., Siddiqi, S. H., Downar, J., Fitzgerald, P. B., & Fox, M. D. (2020). Using brain imaging to improve spatial targeting of transcranial magnetic stimulation for depression. *Biological Psychiatry*.

CIBC. (2015). *Seg3D: Volumetric Image Segmentation and Visualization. Scientific Computing and Imaging Institute (SCI)*. http://www.seg3d.org

Corthout, E., Barker, A., & Cowey, A. (2001). Transcranial magnetic stimulation. *Experimental Brain Research*, *141*(1), 128–132.

Curtin, A., Tong, S., Sun, J., Wang, J., Onaral, B., & Ayaz, H. (2019). A systematic review of integrated functional near-infrared spectroscopy (fNIRS) and transcranial magnetic stimulation (TMS) studies. *Frontiers in Neuroscience*, *13*, 84.

Desikan, R. S., Ségonne, F., Fischl, B., Quinn, B. T., Dickerson, B. C., Blacker, D., Buckner, R. L., Dale, A. M., Maguire, R. P., & Hyman, B. T. (2006). An automated labeling system for subdividing the human cerebral cortex on MRI scans into gyral based regions of interest. *Neuroimage*, *31*(3), 968–980.

Ding, Z., Ouyang, G., Chen, H., & Li, X. (2020). Closed-loop transcranial magnetic stimulation of real-time EEG based on the AR mode method. *Biomedical Physics & Engineering Express*, *6*(3), 035010.

Esposito, R., Bortoletto, M., & Miniussi, C. (2020). Integrating TMS, EEG, and MRI as an approach for studying brain connectivity. *The Neuroscientist*, *26*(5–6), 471–486.

Esteban, O., Markiewicz, C. J., Blair, R. W., Moodie, C. A., Isik, A. I., Erramuzpe, A., Kent, J. D., Goncalves, M., DuPre, E., & Snyder, M. (2019). fMRIPrep: A robust preprocessing pipeline for functional MRI. *Nature Methods*, *16*(1), 111–116.

FDA. (2020). *Neuronal Navigator* (21 CFR 882.4560) [Computer software]. https://www.accessdata.fda.gov/cdrh_docs/pdf19/K191422.pdf

Goetz, S. M., Kozyrkov, I. C., Luber, B., Lisanby, S. H., Murphy, D. L., Grill, W. M., & Peterchev, A. V. (2019). Accuracy of robotic coil positioning during transcranial magnetic stimulation. *Journal of Neural Engineering*, *16*(5), 054003.

Gomez, L. J., Dannhauer, M., Koponen, L. M., & Peterchev, A. V. (2020). Conditions for numerically accurate TMS electric field simulation. *Brain Stimulation*, *13*(1), 157–166.

Gomez, L. J., Dannhauer, M., & Peterchev, A. V. (2021). Fast computational optimization of TMS coil placement for individualized electric field targeting. *Neuroimage*, *228*, 117696.

Jenkinson, M., Beckmann, C. F., Behrens, T. E., Woolrich, M. W., & Smith, S. M. (2012). Fsl. *Neuroimage*, *62*(2), 782–790.

Jung, J., Bungert, A., Bowtell, R., & Jackson, S. R. (2020). Modulating brain networks with transcranial magnetic stimulation over the primary motor cortex: A concurrent TMS/fMRI study. *Frontiers in Human Neuroscience*, *14*, 31.

Kammer, T., Beck, S., Thielscher, A., Laubis-Herrmann, U., & Topka, H. (2001). Motor thresholds in humans: A transcranial magnetic stimulation study comparing different pulse waveforms, current directions and stimulator types. *Clinical Neurophysiology*, *112*(2), 250–258.

MathWorks. (2018). *MATLAB* (9.4.0.813654 (R2018a)) [MacOS]. The MathWorks Inc. https://www.mathworks.com/products/matlab.html

Nummenmaa, A., McNab, J. A., Savadjiev, P., Okada, Y., Hämäläinen, M. S., Wang, R., Wald, L. L., Pascual-Leone, A., Wedeen, V. J., & Raij, T. (2014). Targeting of white matter tracts with transcranial magnetic stimulation. *Brain Stimulation*, *7*(1), 80–84.

Opitz, A., Fox, M. D., Craddock, R. C., Colcombe, S., & Milham, M. P. (2016). An integrated framework for targeting functional networks via transcranial magnetic stimulation. *Neuroimage*, *127*, 86–96.

Ruohonen, J., & Karhu, J. (2010). Navigated transcranial magnetic stimulation. *Neurophysiologie Clinique/Clinical Neurophysiology*, *40*(1), 7–17.

Rusjan, P. M., Barr, M. S., Farzan, F., Arenovich, T., Maller, J. J., Fitzgerald, P. B., & Daskalakis, Z. J. (2010). *Optimal transcranial magnetic stimulation coil placement for targeting the dorsolateral prefrontal cortex using novel magnetic resonance image-guided neuronavigation*. Wiley Online Library.

Schönfeldt-Lecuona, C., Thielscher, A., Freudenmann, R. W., Kron, M., Spitzer, M., & Herwig, U. (2005). Accuracy of stereotaxic positioning of transcranial magnetic stimulation. *Brain Topography*, *17*(4), 253–259.

Silva, L. M., Silva, K. M. S., Lira-Bandeira, W. G., Costa-Ribeiro, A. C., & Araújo-Neto, S. A. (2020). Localizing the primary motor cortex of the hand by the 10-5 and 10-20 systems for neurostimulation: An MRI study. *Clinical EEG and Neuroscience*, 1550059420934590.

Smith, J. E., & Peterchev, A. V. (2018). Electric field measurement of two commercial active/sham coils for transcranial magnetic stimulation. *Journal of Neural Engineering*, *15*(5), 054001.

Thielscher, A., Antunes, A., & Saturnino, G. B. (2015). Field modeling for transcranial magnetic stimulation: A useful tool to understand the physiological effects of TMS? *2015 37th Annual International Conference of the IEEE Engineering in Medicine and Biology Society (EMBC)*, 222–225.

Thut, G., Bergmann, T. O., Fröhlich, F., Soekadar, S. R., Brittain, J.-S., Valero-Cabré, A., Sack, A. T., Miniussi, C., Antal, A., & Siebner, H. (2017). *Guiding transcranial brain stimulation by EEG/MEG to interact with ongoing brain activity and associated functions*.

Voyvodic, J. T. (1999). Real-time fMRI paradigm control, physiology, and behavior combined with near real-time statistical analysis. *Neuroimage*, *10*(2), 91–106.

Wang, J. X., Rogers, L. M., Gross, E. Z., Ryals, A. J., Dokucu, M. E., Brandstatt, K. L., Hermiller, M. S., & Voss, J. L. (2014). Targeted enhancement of cortical-hippocampal brain networks and associative memory. *Science*, *345*(6200), 1054–1057.

Zhang, B., Liu, J., Bao, T., Wilson, G., Park, J., Zhao, B., & Kong, J. (2020). Locations for noninvasive brain stimulation in treating depressive disorders: A combination of meta-analysis and resting-state functional connectivity analysis. *Australian & New Zealand Journal of Psychiatry*, *54*(6), 582–590.

Zrenner, C., Belardinelli, P., Müller-Dahlhaus, F., & Ziemann, U. (2016). Closed-loop neuroscience and non-invasive brain stimulation: A tale of two loops. *Frontiers in Cellular Neuroscience*, *10*, 92.